3-2018

Correlation for Sessile Drop Evaporation Over a Wide Range of Drop Volatilities, Ambient Gases and Pressures

Peter Kelly-Zion
Trinity University, plkelly@trinity.edu

Christopher J. Pursell
Trinity University, cpursell@trinity.edu

Gregory N. Wassom
Trinity University, gwassom@trinity.edu

Brenton V. Mandelkorn
Trinity University, bmandelk@trinity.edu

Chris Nkinthorn
Trinity University, cnkintho@trinity.edu

Repository Citation

P.L. Kelly-Zion, C.J. Pursell, G.N. Wassom, B.V. Mandelkorn, C. Nkinthorn, "Correlation for sessile drop evaporation over a wide range of drop volatilities, ambient gases and pressures," International Journal of Heat and Mass Transfer, 118 (2018) pp. 355-367. https://doi.org/10.1016/j.ijheatmasstransfer.2017.10.129

https://doi.org/10.1016/j.ijheatmasstransfer.2017.10.129.
Published version may be obtained at https://authors.elsevier.com/a/1W11G_Q5zCHtK for free until Dec. 29, 2017.

Correlation for Sessile Drop Evaporation Over a Wide Range of Drop Volatilities, Ambient Gases and Pressures

P.L. Kelly-Zion[a,*], C.J. Pursell[b], G.N. Wassom[a], B.V. Mandelkorn[a], C. Nkinthorn[a]

[a] Department of Engineering Science

Trinity University, San Antonio 78212, United States

[b] Department of Chemistry

Trinity University, San Antonio 78212, United States

Abstract

A correlation for the evaporation of sessile drops over a very broad range of conditions was developed based on measured evaporation rate data obtained for drops of acetone, methanol, and six hydrocarbons ranging from hexane to isooctane, evaporating in air, helium, argon, and krypton, over a range of ambient pressures from 96 kPa to 615 kPa. The experiments were designed to produce a large variation in the rates of diffusion and buoyancy-induced (natural) convection of the vapor phase amongst the experimental conditions. The correlation, which fits the measurements with an RMS relative error of 5.2%, is a simple equation involving conventional parameters for diffusive and convective transport and is applicable to conditions for which vapor transport limits the rate of evaporation. Application of the correlation requires knowledge of eight basic properties: the ambient pressure and temperature, the equilibrium vapor pressure of the evaporating component, the diffusion coefficient for the evaporating component in the ambient gas, the viscosity of the ambient gas, the radius of the sessile drop, and the molecular weights of the evaporating component and the ambient gas. The correlation is much easier to implement than a computational model based on the coupled conservation equations of mass, energy, and momentum for the two phases, and it offers a single mathematical expression that provides valuable insight into how the roles of diffusive and convective transport change with physical and geometrical parameters. The correlation can be a valuable tool to aid in the analyses of applications involving sessile drop evaporation and to support the validation of complex computational models.

The range of experimental conditions resulted in a large variation in the rates of diffusive and naturally convective transport of the vapor. Over the range of experimental conditions, the liquid volatility, as indicated by the equilibrium vapor pressure, was varied by a factor of 16.7, the mass diffusivity by a factor of 52.2, the density difference ratio (the impetus for natural convection) by a factor of 3,557, and the drop radius by a factor of 22. In terms of the Rayleigh number, the experimental data covers a range from 5 to 361,000. Consequently, the correlation is applicable to a very broad range of conditions. To our knowledge these evaporation rate measurements of sessile drops in gases other than air and at pressures above one atmosphere are the first to be reported in the literature.

Nomenclature

a	correlation constant
b	correlation constant
c	correlation constant
d	correlation constant
D	diffusion coefficient
e	correlation constant
E	mass evaporation rate
f	correlation constant
g	gravitational acceleration
h	correlation constant

[*] Corresponding author: Tel.: 1 210 999 7518; fax: 1 210 999 8037
E-mail address: peter.kelly-zion@trinity.edu (P.L. Kelly-Zion)

H	fraction of the equilibrium vapor concentration in the ambient gas (humidity)
i	correlation constant
j	correlation constant
n	correlation constant
n'	correlation constant
P	ambient pressure
P_v	equilibrium vapor pressure
R	drop radius
R_o	standard drop radius, 1 mm
R_u	universal gas constant
Ra	Rayleigh number
Sc	Schmidt number
Sh	Sherwood number
Sh_D	Sherwood number for diffusion-limited evaporation
T	ambient temperature
z	counter-diffusion correction factor

Greek Symbols

α	thermal diffusivity
θ	contact angle
ρ	mass density
ν	kinematic viscosity
ν_o	kinematic viscosity of the ambient gas at 25°C and 101.3 kPa
φ	relative humidity

Subscripts

a	ambient gas or ambient conditions
C	convective
cor	value computed by the correlation
D	diffusive or diffusion-limited
i	summation index
m	measured value
s	drop surface
v	vapor or equilibrium vapor conditions
∞	ambient condition

Superscripts

*	convection-influenced diffusion or diffusion-influenced convection

1. Introduction

The goal of this study is to develop a correlation for the evaporation of sessile drops under conditions for which the evaporation rate is limited by the rate of vapor transport, and therefore not limited by thermal transport or transport within the liquid drop. The intention is to obtain a simple correlation based on a limited number of physical properties of the drop and the ambient gas that accurately predicts the evaporation rate of drops over a very wide range of conditions. While the detailed characteristics of the vapor transport processes of diffusion and natural convection cannot be determined from the simple correlation, the net effects on the drop evaporation rate can be predicted within a relatively small amount of uncertainty. Thus, a simple correlation may be a desirable alternative to complicated and computationally expensive models based on the fundamental conservation laws. Furthermore, the correlation may provide a form of validation for computational models, which are important for studying the details of the various physical phenomena affecting evaporation. For this purpose, the correlation would provide the expected evaporation rate values which then may be compared with the results of a detailed computational model.

Evaluation of the influences on the evaporation rate of vapor phase diffusion and natural convection is very difficult due to the fact that both of these transport processes affect the vapor density distribution, which, in turn, drives the two transport processes. The effects are evident in Fig. 1, which presents two vapor density distributions in a vertical plane passing through the center of the drop. Fig. 1a shows the computed vapor distribution surrounding a sessile hexane drop of radius 6.5 mm when diffusion is the only mass transport process. This distribution is computed by solving the steady-state Laplace equation [1,2]. By diffusion the vapor moves outward from the drop in all directions creating approximately hemispherical surfaces of constant vapor density. The measured hexane vapor distribution, which is presented in Fig. 1b, is much different and shows the effects of natural convection [3]. The hexane vapor is heavier than the ambient air so the vapor-air mixture near the drop flows along the surface of the substrate radially away from the drop. This radially outward flow along the substrate surface likely sets up a vertically downward flow of air above the drop. As a consequence, the vapor distribution is squished vertically, stretched radially, and diluted by the air. These effects, in turn, affect the diffusive flux distribution, which are computed along the surface of a short cylindrical control volume, shown in red, and are indicated by white arrows over half of the control volume surface. Comparing the two distributions, it is evident that natural convection of the hexane-air mixture results in an increase in the vertical component of the diffusive flux and a reduction of the radial component.

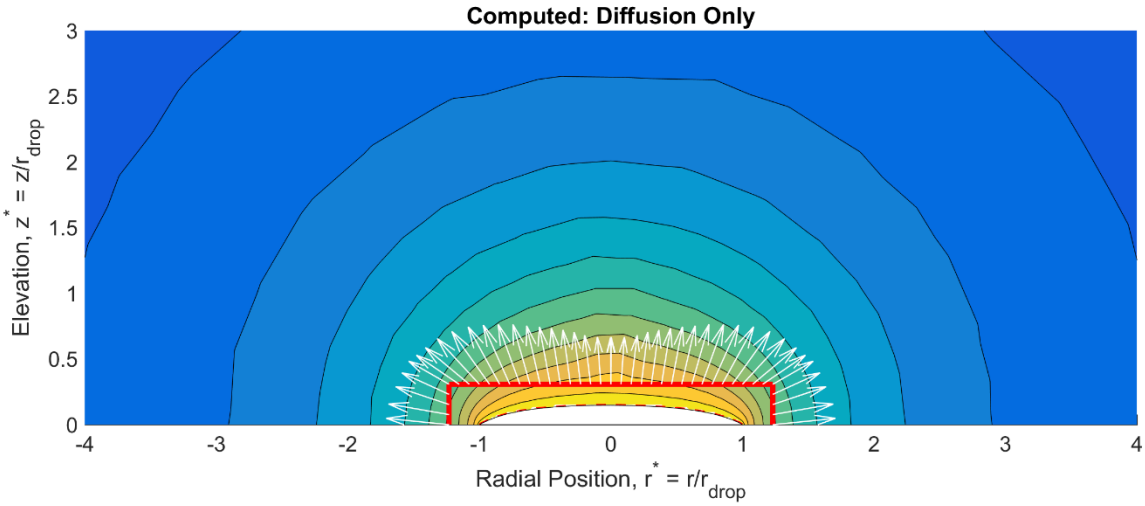

(a)

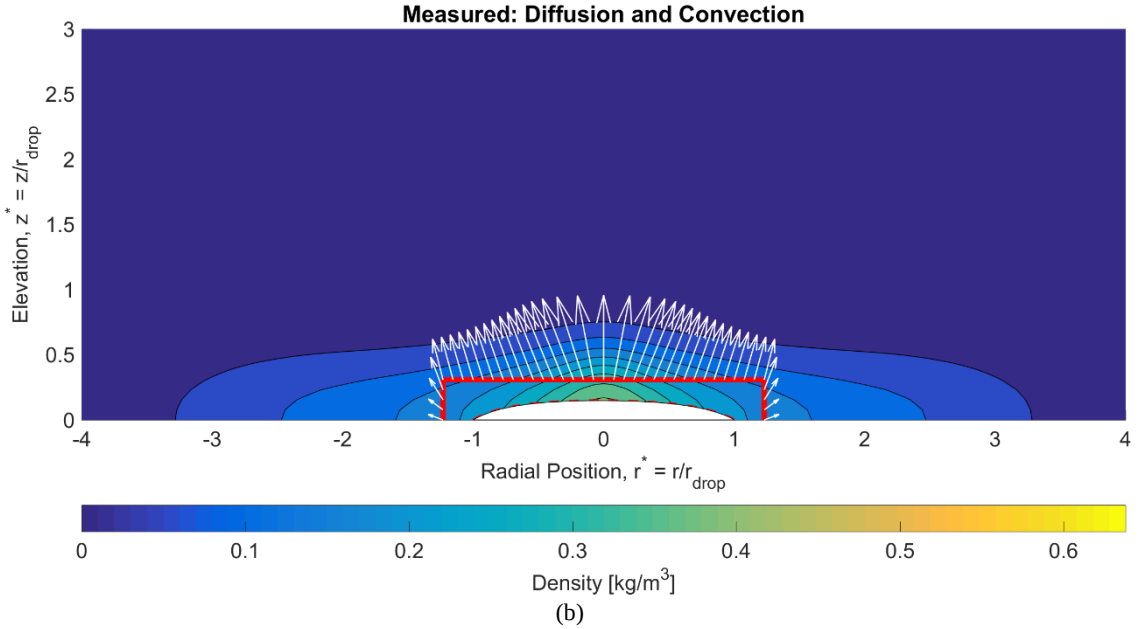

(b)

Figure 1. Comparison of the vapor phase concentration distributions along a vertical plane passing along a diameter of a sessile hexane drop of radius 6.5 mm. Both the radial and vertical coordinates are normalized by the drop radius. Figure 1a presents the vapor phase distribution calculated assuming transport by diffusion only and Fig. 1b presents the measured distribution, which is strongly influenced by natural convection. The profile of the drop is indicated by the red dashed line. The same color map is applicable to both figures. A cylindrical control volume is indicated by the solid red line with the white vectors indicating the diffusive flux along the control surface.

There are two mathematical forms that have been commonly used to correlate natural convection-driven evaporation. Both forms were developed for the evaporation of water. One form, shown in Eq. 1, relates the Sherwood number (*Sh*), which is a dimensionless mass transfer coefficient for evaporation, to the Rayleigh number (*Ra*), which generally represents the relative effects of buoyancy and viscosity. A comprehensive review of published *Sh-Ra* correlations was conducted by Bower and Saylor [4]. The second popular correlation form is the Dalton model. This model relates the evaporation rate to the product of a set of velocity-dependent coefficients and the difference in partial vapor pressures of the evaporating liquid at the drop surface and in the ambient air, and the inverse of the latent heat of evaporation. A review of Dalton-type correlations was conducted by Jodat et al. [5], and they noted the inability of the Dalton based correlations to account for changes in the vapor density difference. Consequently, they proposed a modified Dalton model for natural convection, given by Eq. 2. As discussed in [6] the *Sh-Ra* and the Dalton correlations were applied to a large set of evaporation rate data of hydrocarbons evaporating in air. While neither correlation performed satisfactorily, the *Sh-Ra* correlation performed much better than the Dalton correlation. As a consequence, our efforts to develop a more comprehensive correlation involved expanding and modifying the *Sh-Ra* correlation.

$$Sh = c \cdot Sc^{1/3} Ra^{n} \quad (1)$$

$$E = 0.01c(P_{v,s} - \varphi P_{v,\infty})^{n}(\rho_s - \rho_\infty)^{n'} \quad (2)$$

Previously, empirical models for the combined convective-diffusive evaporation rate were developed by assuming that the evaporation rate is a sum of a diffusive contribution and a convective distribution, i.e. $E = E_D + E_C$ [7-9]. In these models, the diffusive contribution, E_D, is computed according to the solution to the steady-state Laplace equation. In one study, solutal convection (caused by the vapor being heavier than the ambient gas) was considered with negligible thermally-induced convection [7], whereas for the other studies thermally-induced convection was considered with negligible solutal convection [8,9]. Nearly identical correlations were developed both with low RMS relative errors despite differences in data sets and in the expressions used to compute E_D. However, the RMS error increases when the correlation is applied to a data set that represents a broader range of physical conditions. For example, the correlation of [7] results in an RMS relative error of 33% when applied to the data set used to develop the new correlation reported in this paper.

The new correlation fits measurements of two series of experiments which were designed to control the relative effects of vapor phase diffusion and buoyancy-induced convection. In all of the experiments, the drop was contained on a flat aluminum substrate and the drop was pinned by surface tension to a confined area in order to maintain a constant, controlled size as the contact angle reduced in time. In one set of experiments, the rates of evaporation of acetone, methanol, and six hydrocarbons ranging from hexane to isooctane were measured for a broad range of drop radii from 1 to 22 mm. (The large drops are more aptly described as puddles.) This set of experiments was conducted in air at atmospheric pressure. A second set of experiments was conducted for which the drop was placed in a sealed enclosure which enabled the pressure and the ambient gas surrounding the drop to be controlled. The evaporation rates of hexane and methanol, evaporating into four different gases at pressures from 1 to 6 atmospheres were measured. The gases were selected to provide a broad range of diffusivities and of differences between the vapor and gas densities. The ratio of that density difference to the ambient gas density (the density difference ratio) is the impetus for buoyancy-induced convection. The correlation was applied only to cases for which the molecular weight of the evaporating component was greater than or equal to the molecular weight of the ambient gas, and thus the correlation applies only to downward-directed natural convection and not upward convection as occurs when the vapor is lighter than the ambient gas. Taken together, the range of conditions for the two sets of experiments covered a factor of 16.7 variation in liquid volatility as indicated by the equilibrium vapor pressures, a factor of 52.2 variation in mass diffusivities, a factor of 3,557 variation in the density difference ratios, and a factor of 22 variation in drop radii. As a result, the correlation is applicable to a very broad range of conditions. In terms of the Rayleigh number, which is commonly used for correlations involving natural convection, the correlation fits data covering a range from 5 to 361,000. All of the experiments were conducted at room temperature in order to avoid currents in the ambient gas due to thermally-induced natural convection. For all of the experimental conditions the evaporation rate was controlled by the rate of vapor transport, with evaporative cooling having an insignificant effect for all of the liquids studied except possibly methanol, which has a much higher heat of vaporization than the other liquids.

There are two major differences between the new correlation and the conventional *Sh*-*Ra* relation. The first difference is the new correlation reduces to an expression for diffusion-limited evaporation as the density difference ratio tends to zero or when the drop size becomes very small, whereas the conventional relation reduces to zero for those situations. The second major difference is the new correlation separates the Rayleigh number into a product of three dimensionless terms: 1) the density difference ratio, 2) the product of gravity and the cube of the drop radius divided by the square of the kinematic viscosity, gR^3/ν^2, and 3) the Schmidt number, and allows the correlation to have a different dependency for each of these three terms. In contrast, for the conventional correlation, Eq. 1, all three of the terms have the same order of dependency, *n*, since they are contained within the Rayleigh number. The definition of the *Ra* commonly includes the Prandtl number (ν/α), which is appropriate for thermally-induced natural convection, and that is the form used in the correlations reviewed by Bower and Saylor [4]. Since our study pertains to natural convection induced by a non-uniform mass distribution resulting from the vapor distribution, we replaced the Prandtl number with the Schmidt number (ν/D), essentially replacing thermal diffusivity with mass diffusivity in the expression for the Rayleigh number. As a consequence of this replacement, the number of physical properties that the correlation is based on is reduced.

The new correlation predicts the measured evaporation rates to within a root-mean-square (RMS) relative error of 5.2%, which is especially good considering the very broad range of conditions, and is a great improvement over the conventional correlation, which has an RMS relative error of 16.6% for the same data.

2. Methods

The correlation was developed based on evaporation rate measurements taken for a broad range of conditions, from conditions for which vapor transport is expected to be dominated by diffusion to conditions for which vapor transport is expected to be dominated by natural convection. The data were compiled from two sets of experiments. For one set of experiments the drop radius and the liquid component were varied. This set of experiments, labeled Radius/Component (R/C) experiments, was conducted in air at 23.2 ± 0.6°C and 96 kPa. The second set of experiments was conducted using a variety of ambient gas pressures and ambient gases and is labeled Pressure/Gas (P/G) experiments. The P/G experiments were conducted at a temperature of 21.6 ± 0.6°C and at pressures from 96 to 615 kPa. Both sets of experiments were conducted under room temperature conditions to avoid thermally-induced natural convection so that only solutal convection, caused by the vapor being

heavier than the ambient gas, was potentially active. When determining the thermophysical properties for a given measurement condition, the specific temperature measured during each experiment was used.

2.1 Experimental methods

The evaporation rates of pinned, sessile drops on an aluminum substrate were measured. The substrate contains a slightly elevated disk-shaped platform on which the drop was formed, with the drop attaching to the edge of the platform and thereby being pinned in place by the surface tension force. In this way the radius of the platform controls the radius of the drop, i.e. the radius of the contact area. This configuration is shown schematically in Fig. 2. As the drop evaporates, eventually it pulls from the edge of the platform and the drop radius reduces. The evaporation rate measurements only pertain to the period of time when the drop is attached to the edge and thus while the radius is constant.

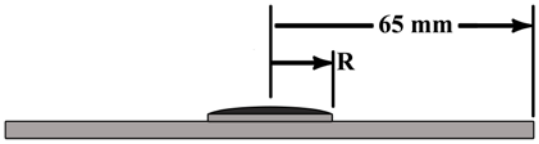

Figure 2. Schematic of a profile view of a drop, shown in black, pinned to the aluminum substrate. The drop radius varied from 1 to 22 mm whereas the substrate radius was fixed at 65 mm.

2.1.1 Radius/Component (R/C) Experiments

The evaporation rates in air at room temperature of acetone, methanol, and six hydrocarbons ranging from hexane to isooctane were measured for drops of radius from 1 to 22 mm. The procedure for this set of experiments is discussed in reference [7]. For drops having a radius greater than 2 mm, the evaporation rates were measured using an analytical balance to record the changing mass with time. The evaporation rates of drops having a radius of 1 or 2 mm were measured using a shadowgraph imaging technique since the relatively slow evaporation rates of these small drops caused complications when using the analytical balance. As discussed in [7], the two techniques yielded results that differ by less than 7%. The initial volume of the drop was controlled and resulted in contact angles that, for drop radii greater than 4 mm, varied approximately from 28° to 21° during a measurement. Using as a guide Hu and Larson's expression for diffusion-limited evaporation, given in Eq. 3, this variation in the contact angle is expected to result in about a 2% variation in the evaporation rate, which is considered small relative to measurement uncertainties [1]. In Eq. 3, H is the fraction of the equilibrium vapor mass concentration in the ambient gas far from the drop, which was zero for our experiments. As discussed in [7], for drops larger than 2 mm in radius, the measured evaporation rate was approximately constant, indicating that the effects of a changing contact angle and, potentially, of evaporative cooling were negligible. For the smallest drops (R = 1 mm) the contact angle was as high as 50° and decreased to approximately 10° during evaporation. For this range of angles, Eq. 3 predicts a 14% variation in the evaporation rate. The maximum variation in the measured evaporation rate during a single test was 20% and occurred for the smallest drop (1 mm) of the most volatile component (3-methylpentane). For each experimental condition, at least three and generally five measurement trials were performed.

$$E = \pi R D (1 - H) \rho_v (0.27\theta^2 + 1.30) \quad (3)$$

The eight hydrocarbon components and their relevant physical properties are given in Table 1. The term $(\rho_m - \rho_a)/\rho_a$ is the ratio of the difference between the mass density of the vapor-air mixture near the surface of the drop and the ambient gas density $(\rho_m - \rho_a)$ to the ambient gas density, ρ_a. This term, which is called the density difference ratio, represents a driving factor for buoyancy-induced convection.

Table 1. Thermophysical properties of the components used for the R/C set of experiments in air at 23.2°C and 96 kPa. The equilibrium vapor pressure, P_v, is computed according to the Antoine Equation [10] and diffusivity, D, is computed according to the method of Fuller et al. given in [11].

Component	**Acetone**	**3MP**	**Hexane**	**Methanol**	**Cyclohexane**	**Isooctane**	**Heptane**	**Octane**
P_v **[kPa]**	28.4	22.0	18.8	15.4	12.0	6.06	5.61	1.71
D **[mm^2/s]**	11.1	8.00	8.00	16.7	8.16	6.86	7.36	6.86
$(\rho_m - \rho_a)/\rho_a$	0.30	0.45	0.39	0.017	0.24	0.19	0.14	0.052

2.1.2 Pressure/Gas (P/G) Experiments

This set of experiments utilized an aluminum pressure chamber to allow different pressures and ambient gases to be used in order to broaden the ranges of influence of diffusion and natural convection on the evaporation process by varying the gas diffusivity and the density difference ratio. The drop radius was 6 mm for all of these experiments. The pressure chamber, shown in Fig. 3, has an interior volume of approximately 9 L and contains two side windows. Since an analytical balance could not be used with the pressure chamber to measure the evaporation rate, all of the P/G experiments were conducted using the shadowgraph imaging technique. The sessile drop was generated in the closed chamber by passing the needle of a syringe pump through the top of the chamber and injecting the component directly onto the aluminum substrate. The evaporation rates of hexane and methanol were measured under ambient gas pressures from 1 to 6 atm. Table 2 lists the ambient gases used and the diffusivities and the density difference ratios at 21.6°C and 96 kPa. Both diffusivity and density difference ratio are inversely dependent on pressure. For all experiments the molecular weight of the drop component was greater than that of the ambient gas so that convection occurred only in the downward direction.

Figure 3. Photo of the pressure chamber in which the P/G experiments were conducted. The drop evaporation rate was measured using the shadowgraph technique through the side windows.

Table 2. Diffusivity and density difference ratio at 21.6°C and 96 kPa for the various component-gas combinations used for the P/G experiments. Methanol evaporation was studied only in helium and air.

Gas	**Helium (4 g/mol)**		**Air (29 g/mol)**		**Argon (40 g/mol)**		**Krypton (84 g/mol)**	
Component	D [mm^2/s]	$(\rho_m-\rho_a)/\rho_a$	D [mm^2/s]	$(\rho_m-\rho_a)/\rho_a$	D [mm^2/s]	$(\rho_m-\rho_a)/\rho_a$	D [mm^2/s]	$(\rho_m-\rho_a)/\rho_a$
Hexane (86 g/mol)	27.31	3.70	7.92	0.36	7.38	0.21	5.37	0.0051
Methanol (32 g/mol)	56.77	1.02	16.54	0.015	–	–	–	–

To prepare an experiment, a vacuum pump evacuated the pressure chamber down to a pressure of approximately 10 kPa and then the chamber was filled with the desired ambient gas. This pump-fill cycle was repeated until the residual gas was reduced to about 1% of the desired ambient gas.

2.3 Correlation Development

To successfully correlate the evaporation rate data, it is important both to include the important physical and geometric parameters and to use a function that can approximate the measured data. The R/C data had been correlated previously using a modified form of the *Sh-Ra* relationship given in Eq. 1 [6]. However, this correlation does not adequately predict the evaporation rates over the expanded range of the P/G data. As a consequence, we refined our basic premise regarding the general form of the correlation function. The fundamental ideas which guide our development of the correlation are:

- Whereas there are many complex details that influence evaporation behavior, the net effect on the evaporation rate of a sessile drop can be predicted based on the drop radius, a small number of thermophysical properties, and the ambient temperature and pressure.
  - For conditions for which thermal energy transfer does not limit the evaporation process, the evaporation rate of a pure sessile drop is controlled by the vapor transport mechanisms of convection and diffusion.
- Convection and diffusion are coupled.

    - As Fig. 1 shows, convection can greatly influence the vapor concentration distribution and thereby affect the diffusive flux, which is proportional to the gradient in the vapor concentration.
        - Convection of the heavy vapor causes the vapor distribution to become squished vertically and spread out radially. In this way, the vertical concentration gradients may be increased and the radial gradients may be reduced by convection's influence on the vapor distribution.
    - Diffusion spreads out the vapor distribution and thereby reduces the density difference ratio, which is the impetus for buoyancy-induced convection.
    - The term representing the strength of convection should be moderated by parameters for diffusion. Likewise, the term representing the strength of diffusion should be moderated or promoted by parameters for convection.
- The strength of convection is indicated by the Rayleigh number.
    - As the Rayleigh number tends to zero, suggesting a lack of convection, the correlation should reduce to a purely diffusive evaporation rate.
    - As was shown to be helpful in our previous correlation [6], we allow the Rayleigh number to be split into its dimensionless components and allow each dimensionless component to influence the correlation independently. Thus while $Ra = GrSc = \left[\frac{(\rho_m - \rho_a)}{\rho_a}\right]\left[\frac{gR^3}{\nu^2}\right]\left[\frac{\nu}{D}\right]$, each parameter in brackets is allowed to influence the correlation independently.
- To keep the correlation function simple, the diffusion-limited evaporation rate is modeled using the Weber's disk equation, given by Eq. 4, which is the solution to the steady-state Laplace equation for a circular disk [12]. The factor z is a counter-diffusion correction factor which accounts for the rate of diffusion of the ambient gas in the opposite direction as that of the vapor.
    - The Weber's disk equation is independent of the contact angle.
    - The Weber's disk equation is equivalent to the equation for a spherical cap, Eq. 3, under the limiting case of a contact angle equal to 0 radians and no background vapor in the ambient gas ($H = 0$).
    - As the drop size increases, the drop flattens and the shape approaches a flat disk.
- The evaporation rate is equal to the sum of the diffusive and the convective vapor transports and so the correlation should be a sum of two terms, one which represents convection-influenced diffusion and the other which represents diffusion-influenced convection.

$$E_D = \frac{4RDM_vP_v}{R_uT} z = 4RD\rho_v \left(\frac{P}{P_v}\right) Ln\left[1/(1 - P_v/P)\right] \quad (4)$$

The Sherwood number (*Sh*), which is a dimensionless evaporation rate, was correlated with dimensionless parameters from the Rayleigh number, as discussed above. *Sh* was computed according to Eq. 5. The correlation includes a "diffusive Sherwood number", Sh_D, which is also computed by Eq. 5 but using the diffusion-limited evaporation rate, E_D, given by Eq. 4 instead of the overall evaporation rate, *E*.

$$Sh = \frac{h_m R}{D} = \frac{ER_uT}{\pi RDP_vM} \quad (5)$$

Different functional forms were used to fit the measured data and the quality of the fit was assessed by computing the root mean square (RMS) relative error according to Eq. 6. Following the previous success of power-law correlations, e.g. Eq. 1, all of the correlation functions investigated were a combination of power-law functions, that is a sum of products of parameters that are each raised to a power. To fit the measured data, the set of coefficients and exponents that produce the closest fit for the given correlation function was computed using a nonlinear fitting routine in Matlab©. As the number of correlation fitting parameters increases, the RMS relative error reduces at a continuously diminishing rate, as shown in Fig. 4. Using more than eight parameters provides very little improvement in the fit. Therefore, with the goal of keeping the correlation simple while still capturing the net effects of the detailed physics, the eight-parameter correlation is deemed the best balance of simplicity and accuracy. Included in Fig. 4 for reference is the RMS relative error of the four-parameter correlation that was previously developed for the R/C data and applied to the set of R/C and P/G data [6]. Clearly, more than four parameters are needed to accurately correlate the very broad range of conditions resulting from varying the ambient gas and pressure in addition to varying the drop size and component.

$$RMS\ Relative\ Error = \sqrt{\frac{1}{N}\sum_i^N \left[\frac{(E_{c,i} - E_{m,i})}{E_{m,i}}\right]^2} \quad (6)$$

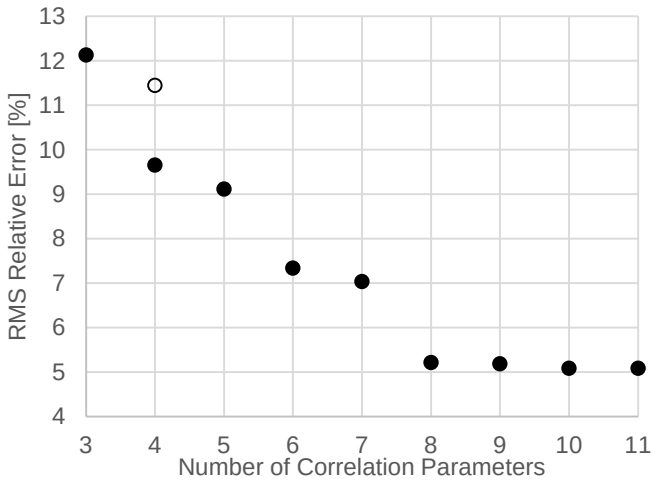

Figure 4. Correlation error as a function of the number of correlation parameters. The open symbol indicates the error that results when applying the correlation that had been developed for the R/C subset of data, ref. [6], to the combined R/C and P/G data set.

3. Results

3.1 Measurement Results

The measured evaporation rates for the R/C and P/G data are presented in Fig. 5. Each datum point represents the average of at least 3 measurements. Figure 5a presents the evaporation rates of the R/C data set and shows the dependence on the thermophysical properties of the liquid drop and the strong, nonlinear dependence on drop size. For example, as the drop radius increases from 1 to 22 mm, the evaporation rates of 3MP and heptane increase by factors of 79 and 65, respectively. The effects of ambient gas and pressure are presented in Fig. 5b for the P/G data set. The evaporation rate is shown to decrease as either the ambient pressure or the molecular weight of the ambient gas increases. Considering the two data sets, eighty-one different measurement conditions were tested.

The measured evaporation rates are generally much greater than the rates computed for diffusion-limited evaporation, as shown for hexane in Fig. 6. The discrepancy is attributed to vapor phase convection. Figure 6a compares the measured and diffusion-limited rates as a function of drop radius at 23.2°C and 96 kPa. As is well known, the diffusion-limited evaporation rate is linear with respect to drop radius but the measured evaporation rate is approximately proportional to the radius raised to the power 1.4.

The effect of ambient pressure on hexane evaporation for a 6 mm drop in air is presented in Fig. 6b. The diffusion-limited evaporation rate is inversely proportional to the ambient pressure whereas the measured rate reduces more slowly with pressure and is approximately proportional to pressure raised to the power -3/4.

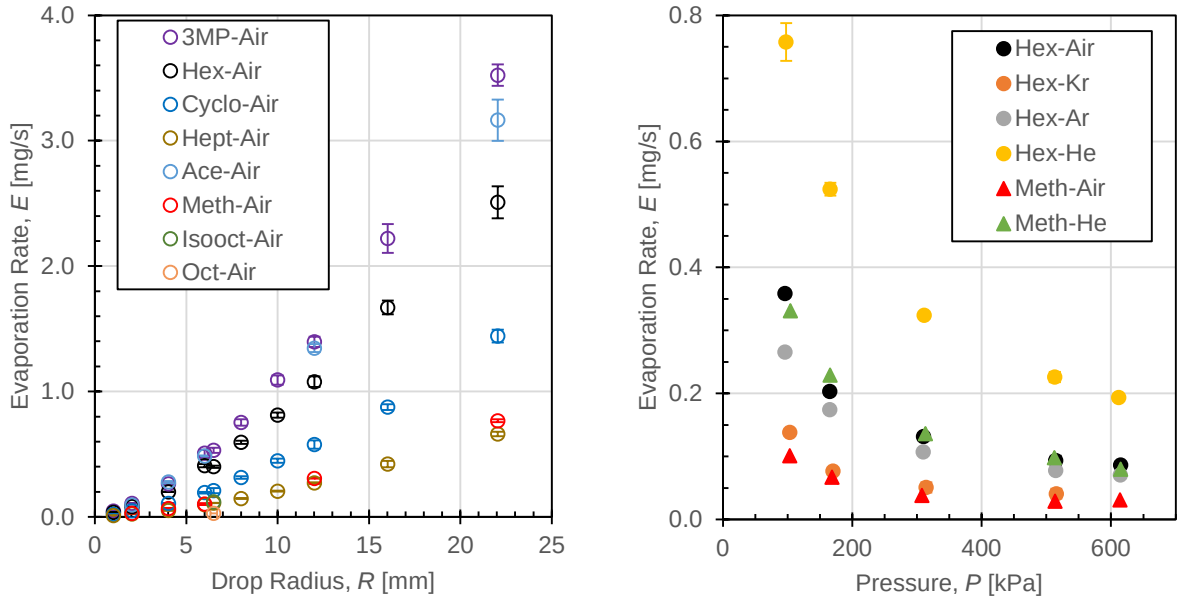

(a) R/C Data Set

(b) P/G Data Set

Figure 5. Measured evaporation rate data from the R/C experiments (a) and the P/G experiments (b). The R/C experiments were conducted in air at 23.2 ± 0.6°C and 96 kPa, and the P/G experiments were conducted at 21.6 ± 0.6°C with a constant drop radius equal to 6 mm. Error bars representing ± 1 standard deviation are included, though for many experiments the error bars are shorter than the datum symbol.

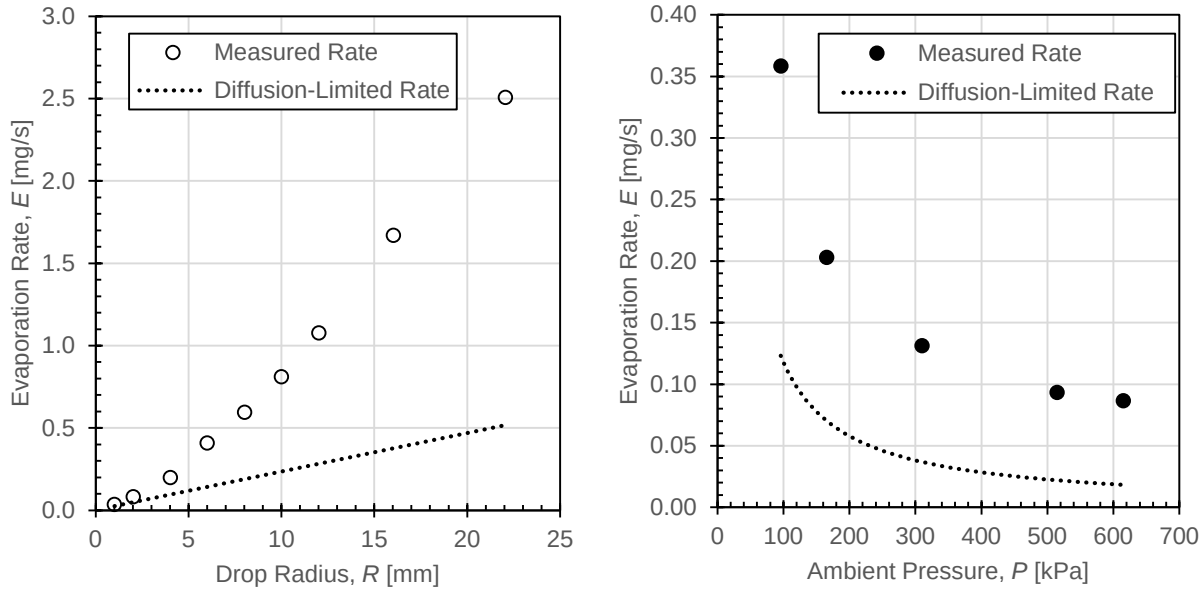

(a)

(b)

Figure 6. Comparison of measured and diffusion-limited evaporation rates of hexane in air. Figure 6a presents the comparison as a function of drop size in air at 96 kPa and 23.2°C, and Fig. 6b presents the comparison for a 6 mm drop as a function of ambient pressure at 21.3°C.

3.2 Correlation Results

The eight-parameter correlation which fits the measured data with an RMS relative error of 5.2% is given by Eq. 7, with the values of the coefficients and exponents provided in Table 3. As desired, the correlation reduces to a diffusion-limited evaporation rate, represented by Sh_D, as the density difference ratio tends to zero and thus as convection becomes negligible. The

right-hand side of Eq. 7 is composed of two terms, the first representing convection-influenced diffusion, Sh_D^*, and the second representing diffusion-influenced convection, Sh_C^*.

$$Sh_{cor} = Sh_D\left\{1 + a\left[\left(\frac{gR^3}{\nu^2}\right)/\left(\frac{gR_o^3}{\nu_o^2}\right)\right]^b\left[\left(\frac{\rho_m-\rho_a}{\rho_a}\right)Sc\right]^c\right\} + dSc^e\left(\frac{\rho_m-\rho_a}{\rho_a}\right)^f\left(\frac{gR_o^3}{\nu^2}\right)^i\left(\frac{gR^3}{\nu_o^2}\right)^j = Sh_D^* + Sh_C^* \qquad (7)$$

Table 3. Values for the coefficients and exponents of the correlation given in Eq. 7.

a	*b*	*c*	*d*	*e*	*f*	*i*	*j*
1.23×10^{-3}	6.48×10^{-1}	-1.40×10^{-1}	8.44×10^{-2}	7.37×10^{-1}	4.78×10^{-1}	3.75×10^{-1}	2.12×10^{-1}

During development of this correlation, it was determined that the term gR^3/ν^2, which is a component of the Rayleigh number and is the only size-dependent term, is unable to provide the proper size dependency over the broad range of ambient pressures and for the variety of ambient gases due to the term's dependence on kinematic viscosity, ν. To provide increased flexibility in the manner in which the correlation is dependent on drop size and viscosity (i.e. ambient pressure and gas), a nominal drop radius, R_o, equal to 1 mm, and a nominal kinematic viscosity, ν_o, equal to the ambient gas viscosity at the standard condition of 25°C and 101.3 kPa are used to generate the terms gR_o^3/ν_o^2, gR_o^3/ν^2 and gR^3/ν_o^2. Each of these terms have different fundamental dependencies. The term gR_o^3/ν_o^2 depends only on the type of ambient gas, the term gR_o^3/ν^2 depends on both the type of ambient gas and the ambient pressure (as well as temperature, which was relatively constant for all of our experiments), and the term gR^3/ν_o^2 depends on the drop size and the type of ambient gas.

The accuracy of the correlation is addressed by Fig. 7, which presents the correlation's relative error at each measurement condition as a function of the "measured" Sherwood number, Sh_m. The correlation fits 78 of the 81 measurements to within ±10% relative error, and 54 of the measurements to within ±5% relative error. The largest error occurs for cases in which the molar mass of the drop component nearly equals that of the ambient gas, i.e. for methanol-air and hexane-krypton combinations. These combinations have the lowest density difference ratios and thus convective transport is expected to be lowest for them. The RMS relative error for each component-gas combination over the range of experimental conditions is given in Table 4. The relative error is of the same order of magnitude for each of the component-gas combinations and, as Fig. 7 shows, the error is generally scattered with positive and negative values and no significant trends.

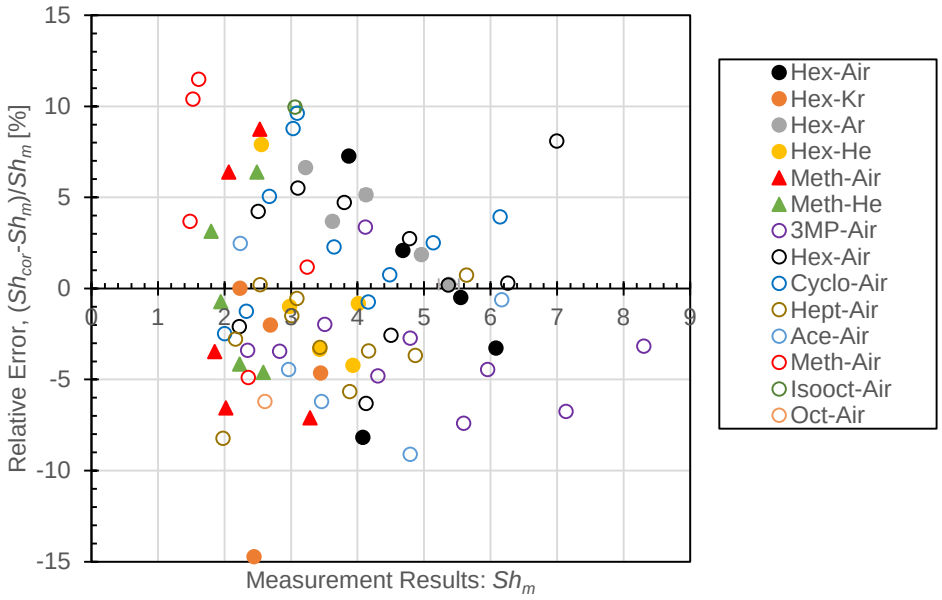

Figure 7. Percent relative error as a function of the dimensionless measured evaporation rate, Sh_m. The solid symbols are data from the P/G experiments and the open symbols are data from the R/C experiments.

Table 4. Percent RMS relative error for each of the component-gas combinations. Note that only one measurement was taken for the isooctane-air and octane-air combinations.

Radius/Component Data		**Pressure/Gas Data**	
3MP-Air	4.5%	Hexane-Air	5.2%
Hexane-Air	4.4%	Hexane-Krypton	7.8%
Cyclohexane-Air	4.8%	Hexane-Argon	4.2%
Heptane-Air	3.8%	Hexane-Helium	4.3%
Acetone-Air	5.4%	Methanol-Air	6.7%
Methanol-Air	7.5%	Methanol-Helium	4.2%
Isooctane-Air	10.0%		
Octane-Air	6.2%		

Over the broad range of measurement conditions, the correlation predicts the evaporation rate very well, as shown in Fig. 8, which compares the evaporation rates computed by the correlation to the measured evaporation rates. Figure 8a shows the evaporation rate as a function of drop radius for the different components (R/C data) and Fig. 8b shows the evaporation rate as a function of ambient pressure and gas for hexane and methanol drops (P/G data). An expanded view for small drop sizes is presented for acetone and methanol drops in Fig. 9, which includes evaporation rate measurements by Dunn et al. [13]. Although the ambient conditions are approximately the same, the evaporation rates of acetone measured by Dunn et al. are noticeably lower than our measurements. Consequently, while the correlation predicts all of the methanol measurements and our acetone measurements well, the acetone measurements of Dunn et al. fall below the predicted values of the correlation.

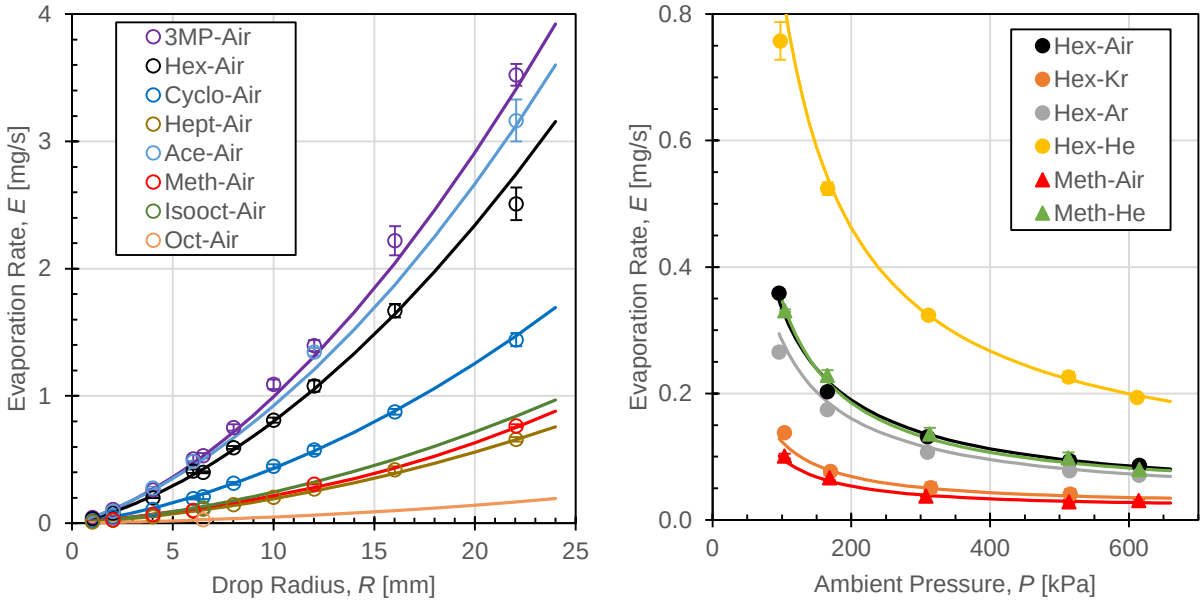

(a) R/C Data Set (b) P/G Data Set

Figure 8. Measured and computed evaporation rates. Measured values are given by the datum symbols and the computed values by the lines. Figure 8a presents the comparison of measured and computed evaporation rates for the R/C data as a function of drop radius and Fig.8b presents the comparison for the P/G data as a function of ambient pressure.

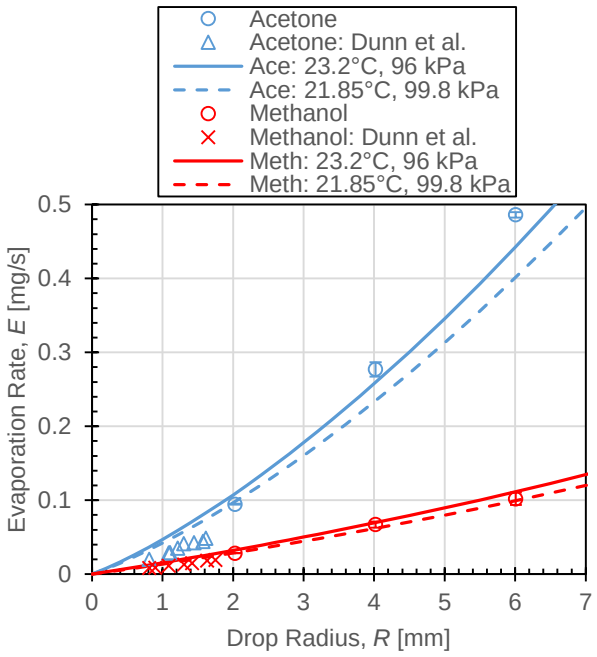

Figure 9. Expanded view of the measured and computed evaporation rates of acetone and methanol in air for small drop sizes. The measurements of Dunn et al. [13] are included for comparison. The experiments of Dunn et al. were conducted at 21.85°C and 99.8 kPa, a slightly lower temperature and higher pressure than those of the current experiments (23.2°C, 96 kPa). The lines indicate computed values based on the correlation at the two temperature-pressure conditions.

3.3 Coupling of Diffusive and Convective Transport

Having developed a correlation based on the premise that diffusive and convective transport are coupled, we can now use the correlation to investigate the manner by which the two transport mechanisms are predicted to influence each other.

The terms in the convection-influenced diffusion term, Sh_D^*, and those in the diffusion-influenced convection term, Sh_C^*, may be arranged to provide functions of *Ra* as given by Eqs. 8 and 9. Expressing Sh_D^* in terms of *Ra* helps to elucidate the effect that convection has on the diffusive transport. However, as Eq. 8 indicates, Sh_D^* is a function of multiple factors, not simply a function of *Ra*. The effect of convection to either increase or diminish diffusive transport is expressed as the function within the braces and is referred to as K_D for convenience. When convection acts to increase the rate of diffusion K_D is greater than one and, conversely, when convection acts to reduce the rate of diffusion K_D is less than one.

$$Sh_D^* = Sh_D\left\{1 + a\left(\frac{gR_o^3}{\nu_o^2}\right)^{-b}\left[\left(\frac{\rho_m-\rho_a}{\rho_a}\right)Sc\right]^{c-b}Ra^b\right\} = Sh_D K_D \tag{8}$$

$$Sh_C^* = dSc^e\left(\frac{\rho_m-\rho_a}{\rho_a}\right)^f\left(\frac{gR_o^3}{\nu^2}\right)^i\left(\frac{gR^3}{\nu_o^2}\right)^j = d\left(\frac{gR_o^3}{\nu_o^2}\right)^i\left(\frac{\nu_o}{\nu}\right)^{2(i-j)}Sc^{e-j}\left(\frac{\rho_m-\rho_a}{\rho_a}\right)^{f-j}Ra^j \tag{9}$$

3.3.1 Diffusive Transport

Whereas Fig. 1 qualitatively indicates that the effect of convection on diffusive transport is non-uniform, with diffusive transport increasing in some regions and reducing in others, the correlation suggests that the *net* effect of convection is to increase the diffusive transport. This result is not surprising given the form of the correlation since, as Eq. 8 indicates, the only way that convection could have a diminishing effect on the diffusive rate is if the coefficient *a* were negative, and in that case convection could only have a diminishing effect on the diffusive rate. However, a modified form of Eq. 7 for which the 1 is replaced with a ninth fitting parameter was fit to the data, thus enabling K_D to vary from less than to greater than one. The result of fitting this modified function is essentially equivalent to that of fitting Eq. 7, with the ninth fitting parameter equal to 0.96 (instead of 1), the eight other fitting parameters being nearly equal for the two functions, and the two functions having nearly equal relative RMS error values of 5.22% and 5.19%. As a result of replacing 1 with 0.96, the modified correlation suggests that for some conditions (generally for small drop sizes), convection may have the effect of reducing the net rate of diffusion by up to 4%. A reduction of 4% is very small and it is questionable whether such results truly indicate a slight suppressive effect on the net rate of diffusion and are not just a consequence of slight deficiencies in the ability of the mathematical function to correlate the measured data. For example, to compute Sh_D the simplest expression for diffusion-limited evaporation was chosen, Eq. 4, instead of Eq. 3 or other appropriate expression and the possible inaccuracy introduced by the use of Eq. 4 may account for K_D going slightly less than 1

for the modified correlation. In any case, it can be concluded that the effect of convection on the net rate of diffusion varies from no effect (or possibly a slight reduction) to a substantial increase of up to 200% for the wide range of conditions tested.

To observe the manner in which the correlation suggests that convection influences diffusion, K_D is plotted as a function of *Ra* in Fig. 10. For a given component-gas combination, the *Ra* varies with drop size for the R/C data, represented as solid lines in Fig. 10. Therefore, as drop size increases the correlation suggests that convection acts to increase the rate of diffusion according to an equation of the form αR^{3b} or $\alpha R^{1.94}$ where the coefficient α depends on the component-gas combination and ambient pressure. Thus the correlation suggests that convection affects diffusion in an amount that is approximately proportional to the surface area of the drop. This result appears to be consistent with measurements of the vapor distribution shown in Fig. 1b for which the density gradient near the top surface of the drop is much larger than at the side of the drop and so the net rate of diffusion would appear to be strongly dependent on R^2 in that case.

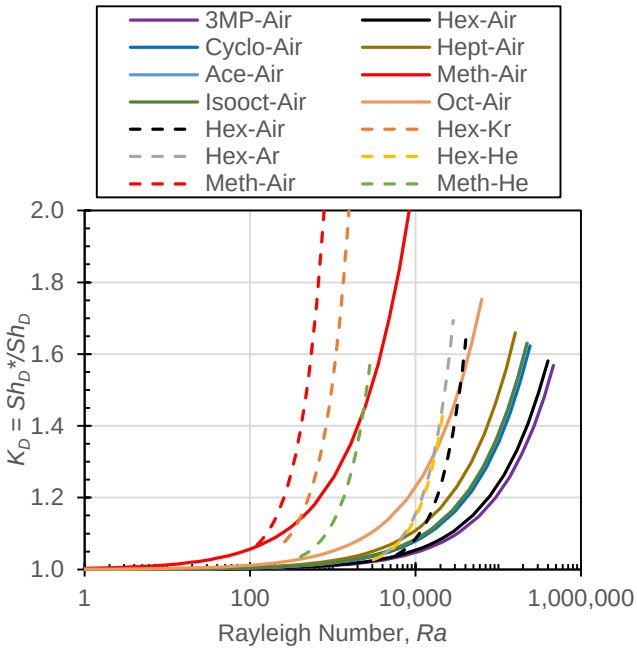

Figure 10. The effect of convection on diffusive transport, K_D, as suggested by the correlation. The solid lines represent R/C data and the dashed lines represent P/G data.

For a constant drop size, the effect of ambient pressure may be seen in the trends given by the dashed lines in Fig. 10, which represent the P/G data. *Ra* is proportional to ambient pressure and consequently the correlation suggests that convection acts to increase the rate of diffusive transport according to an equation of the form βP^{2b-c} or $\beta P^{1.44}$ where the coefficient β depends on the component-gas combination and the drop size.

It should be observed that K_D is not the magnitude of the diffusive transport, rather K_D represents the influence of convection to either increase or decrease the rate of diffusive transport. From the definition of *Sh* given by Eq. 5, the magnitude of diffusive transport, E_D^*, may be expressed as Eq. 10.

$$E_D^* = Sh_D^* \frac{\pi RDP_v M_v}{R_u T} = K_D \frac{4RDM_v P}{R_u T} Ln\left[1/(1 - P_v/P)\right] \quad (10)$$

As is commonly known, when evaporation is diffusion-limited the rate is proportional to the drop size, *R*. The correlation indicates that when convection occurs the diffusive transport rate, E_D^*, is dependent on drop size according to the functional form given by Eq. 11, where the values of the coefficients c_1 and c_2 are positive and depend on the component-gas combination and the ambient pressure. The coefficient c_1 is just equal to E_D/R where E_D is given by Eq. 4. For small drop sizes, convection's influence is negligible and E_D^* is dominated by the first (linear) term. The second term becomes significant only when the drop size becomes large.

$$E_D^* = c_1 R + c_2 R^{2.95} \quad (11)$$

The pressure dependence of E_D^* may be approximated by the form $c_3 P^{-n}$. The value of the coefficient, c_3 and the exponent, *n*, vary for the different component-gas combinations. In all cases pressure acts to reduce the diffusive transport with the strongest effect occurring for the hexane-helium combination ($E_D^* \propto P^{-0.88}$) and the weakest effect for the hexane-krypton combination ($E_D^* \propto P^{-0.67}$).

3.3.2 Convective Transport

Just as the expression for Sh_D^* suggests how convection affects diffusion, the expression for Sh_C^* suggests how diffusion affects convection. Consider the factor $\left[\left(\frac{\nu_o}{\nu}\right)^{2(i-j)} Sc^{e-j}\left(\frac{\rho_m-\rho_a}{\rho_a}\right)^{f-j}\right]$ in Eq. 9. Using the definition of *Sc* and the exponents for the correlation, this factor becomes $\frac{\nu_o^{0.49}\nu^{0.065}}{D^{0.55}}\left(\frac{\rho_m-\rho_a}{\rho_a}\right)^{0.27}$ which indicates the convective transport is moderated approximately according to the inverse square root of the diffusivity, which is a stronger effect than that suggested by the conventional *Sh-Ra* equation, Eq. 1. The expression for Sh_C^* indicates also that the factor Ra^j does not sufficiently account for the influence of the density difference ratio on the rate of convective transport and so the factor $\left(\frac{\rho_m-\rho_a}{\rho_a}\right)^{0.27}$ is included.

Sh_C^* is plotted as a function of *Ra* for all of the measurement conditions in Fig. 11. This plot indicates the dependence of Sh_C^* on *Ra* varies for the different drop component-ambient gas combinations. The dependence on *Ra* is weakest for the methanol-air combination, which has comparatively high diffusivities and generally low density difference ratios, and strongest for the hexane-air and 3MP-air combinations, which have moderate diffusivities and relatively high density difference ratios. The *Ra* dependence of Sh_C^* is moderately strong for combinations such as hexane-helium which have both a high diffusivity and a high density difference ratio. Despite its moderately high density difference ratio, the methanol-helium combination also has a very weak *Ra* dependence due to its very high diffusivity.

For a given component-gas combination at constant pressure, Sh_C^* is proportional to R^{3j} or $R^{0.64}$ and these trends are demonstrated by the solid curves in Fig. 11. Whereas Sh_C^* expresses the relative amount of convective transport to diffusion-limited transport (see Eq. 5), the magnitude of the convective transport, E_C^*, is found to be proportional to $R^{1.64}$, which agrees with the results for the radial dependence of previous models [6-8].

To understand how the proportion of the evaporation rate due to convection varies over the wide range of experimental conditions, plots of Sh_C^*/Sh, which is equal to E_C^*/E, as functions of drop size and ambient pressure are given in Figs. 12a and 12b.

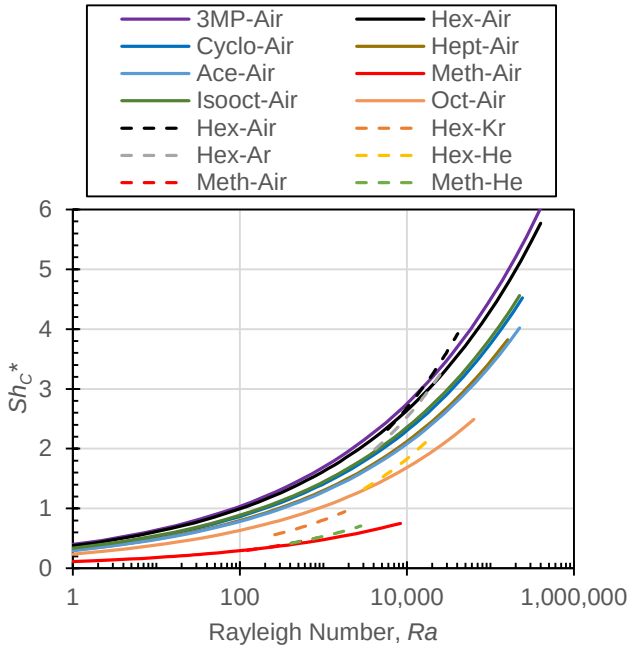

Figure 11. Diffusion-influenced convective transport, Sh_C^*, as a function of *Ra* for all of the measurement conditions. The solid lines represent R/C data and the dashed lines represent P/G data.

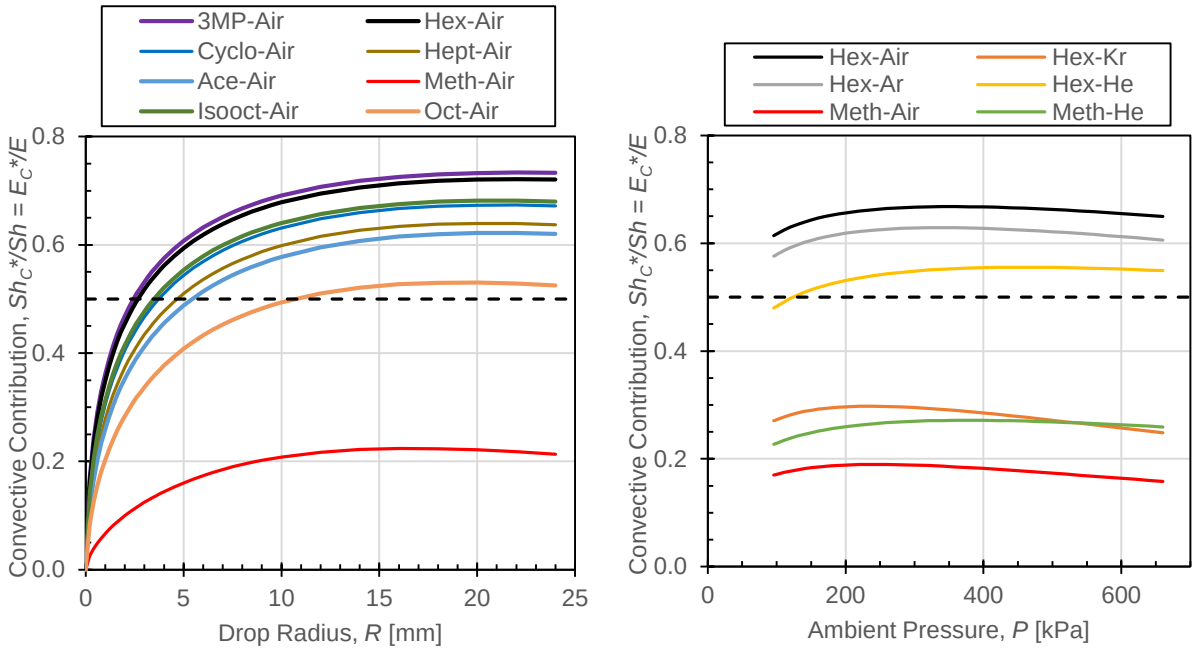

(a) R/C Data Set (b) P/G Data Set

Figure 12. Proportion of the drop evaporation that is attributed to convective transport as predicted by the correlation. Figure 12a presents the convective proportion as a function of drop radius for the R/C components and Fig. 12b presents the proportion as a function of ambient pressure for the P/G combinations. Dashed lines indicate a 50% proportion, i.e. a condition in which convective and diffusive transport are equal.

The evaporation rate of methanol in air was dominated by diffusive transport for all of the measurement conditions, with convection contributing 22% at most for large drops at 96 kPa. The methanol-air combination has both a high diffusivity and a low density difference ratio, two factors that suppress convection. For the smallest methanol drop studied, R = 2 mm, the correlation indicates that the diffusive transport is 9.2 times greater than the convective transport. In other words, convection accounts for just 9.8% of the total evaporation rate.

Of the conditions studied, the evaporation of 3MP into air was most influenced by convection, followed closely by the evaporation of hexane into air. The correlation indicates that convection accounts for up to 73% of the evaporation of large 3MP drops in air and up to 72% of large hexane drops. As mentioned previously, these component-gas combinations have comparatively high density difference ratios and moderate diffusivities.

The type of ambient gas has a strong effect on the relative contributions of convection and diffusion, as shown in Fig. 12b. Comparing the evaporation of hexane in the different ambient gases, convection is greatest in air and smallest in krypton. The density difference ratio, which is the factor that promotes convection, is highest for the hexane-helium combination, but so is the diffusivity and thus its rate of diffusion. As a result, the proportion of convection for hexane-helium is less than that for hexane-air and hexane-argon combinations. For a given drop component, the ranking of convection's proportion of the evaporation rate follows the *Ra*, as expected. However, when comparing different drop components, *Ra* is not sufficient to indicate which has a stronger proportion of convection. For example, for a 6 mm drop at 96 kPa the *Ra* is 410 and the proportion of convection is 23% for methanol in helium whereas the values are 260 and 27% for hexane in krypton.

Whereas the type of ambient gas has a strong effect on the relative contributions of convection and diffusion, ambient pressure has a very small effect, as shown in Fig. 12b. Over the range of ambient pressure from 96 kPa to 660 kPa, convection's proportion of the evaporation rate varies by less than 18%. Thus, increasing the ambient pressure has the effect of reducing the diffusive transport and the convective transport by nominally the same factor. This result suggests that a practical means of controlling the rate of an evaporation process without disturbing the physical processes involved may be to control the ambient pressure.

The correlation results for the proportion of the evaporation rate attributable to convection are in remarkably close agreement with the results of Chen et al.[14], who used a sophisticated computational model to solve the Navier-Stokes equation in both the liquid and gas domains. For a methanol drop of radius equal to 1.75 mm on an aluminum substrate evaporating into air at 1 atm, the model of Chen et al. determined convection's proportion to be 9.7%, which is nearly equal to the value predicted by the correlation for the same conditions, 8.9%. For a 2 mm drop of 3MP under the same conditions, Chen et al. determined that 41% of the evaporation is attributable to convection whereas the correlation indicates the proportion to be 47%.

4. Summary and Conclusions

A correlation for predicting the evaporation rates of sessile drops under a broad range of conditions was developed. The correlation is applicable to drop components having a molecular weight greater than that of the ambient gas and thus for downward-directed natural convection. The fundamental principle on which the correlation was based is that diffusive and convective mass transport are coupled. The correlation provides a means for investigating the nature of the coupling by estimating how one transport mechanism affects the other, and how the magnitude of each transport mechanism varies with the drop size and ambient condition. The primary conclusions based on the correlation are:

- The net effect of convection generally is to increase the rate of diffusion. For the wide range of conditions tested, the effect of convection on the net rate of diffusion varies from approximately no effect to a substantial increase of up to 200%.
- The effect of convection on the diffusive transport is negligible for small drops and becomes significant as the drop size becomes large.
- The convective transport is moderated approximately according to the inverse square root of the diffusivity.
- The magnitude of the convective transport is found to be proportional to $R^{1.64}$.
- Whereas the type of ambient gas has a strong effect on the relative contributions of convection and diffusion, ambient pressure has a very small effect. Increasing the ambient pressure has the effect of reducing the diffusive transport and the convective transport by nominally the same factor.

The success of the correlation in fitting the measured evaporation rates indicates that while multiple complex physical processes are involved in evaporation, the net effect of these processes on the evaporation rate can be predicted based on knowledge of eight physical properties. A significant benefit of the correlation is its simplicity compared to detailed computational models. However, whereas the correlation can successfully predict the net effect of the physical processes involved in evaporation, it cannot replace a detailed computational model for studying those physical processes.

In order to greatly expand the thermophysical conditions of the experiments on which the correlation is based, evaporation rate measurements were conducted at elevated pressures in a variety of ambient gases. To our knowledge these evaporation rate measurements of sessile drops in gases other than air and at elevated pressures are the first to be reported in the literature.

Acknowledgments

Acknowledgment is made to the Donors of the American Chemical Society Petroleum Research Fund for support of this research.

Reference List

[1] H. Hu, R.G. Larson, Evaporation of a Sessile Droplet on a Substrate, J Phys Chem B. 106 (2002) 1334-1344.

[2] B. Sobac, D. Brutin, Triple-Line Behavior and Wettability Controlled by Nanocoated Substrates: Influence on Sessile Drop Evaporation, Langmuir. 27 (2011) 14999-15007.

[3] P.L. Kelly-Zion, C.J. Pursell, N. Hasbamrer, B. Cardozo, K. Gaughan, K. Nickels, Vapor distribution above an evaporating sessile drop. Int. J. Heat Mass Transfer. 65 (2013) 165-172.

[4] S.M. Bower, J.R. Saylor, A study of the Sherwood-Rayleigh relation for water undergoing natural convection-driven evaporation, Int J Heat Mass Transfer. 52 (2009) 3055-3063.

[5] A. Jodat, M. Moghiman, M. Anbarsooz, Experimental comparison of the ability of Dalton based and similarity theory correlations to predict water evaporation rate in different convection regimes, Heat Mass Transfer. 48 (2012) 1397-1406.

[6] P.L. Kelly-Zion, J. Batra, C.J. Pursell, Correlation for the convective and diffusive evaporation of a sessile drop. Int. J. Heat Mass Transfer. 64 (2013) 278-285.

[7] P.L. Kelly-Zion, C.J. Pursell, S. Vaidya, J. Batra, Evaporation of sessile drops under combined diffusion and natural convection. Colloids Surf. , A. 381 (2011) 31-36.

[8] F. Carle, B. Sobac, D. Brutin, Experimental evidence of the atmospheric convective transport contribution to sessile droplet evaporation, Appl Phys Lett. 102 (2013) 061603-1-061603-4.

[9] F. Carle, S. Semenov, M. Medale, D. Brutin, Contribution of convective transport to evaporation of sessile droplets: Empirical model, IJTS. 101 (2016) 35-47.

[10] C.L. Yaws, Thermodynamic and Physical Property Data, Gulf Publishing Company, Houston, TX, 1992.

[11] B.E. Poling, J.M. Prausnitz, J.P. O'Connell, The Properties of Gases and Liquids, 5th ed., McGraw-Hill, New York, 2001.

[12] J. Crank, The Mathematics of Diffusion, 2nd ed., Oxford University Press, New York, 1975.

[13] G.J. Dunn, S.K. Wilson, B.R. Duffy, S. David, K. Sefiane, A mathematical model for the evaporation of a thin sessile liquid droplet: Comparison between experiment and theory, Colloid Surface A. 232 (2008) 50-55.

[14] Y.H. Chen, W.N. Hu, J. Wang, F.J. Hong, P. Cheng, Transient effects and mass convection in sessile droplet evaporation: The role of liquid and substrate thermophysical properties, IJHMT. 108 (2017) 2072-2087.